



Vieta-Fibonacci wavelet-based numerical solutions for population growth models

Jay Kishore Sahani¹, Nikhil Khanna^{2,*}, Gopal Datt³, and Dumitru Baleanu^{4,5}

¹Department of Mathematics, D.A.V. PG College, Siwan, J.P.U., Chapra, India.

²Department of Mathematics, College of Science, Sultan Qaboos University, P. O. Box 36, Al-Khod 123, Muscat, Sultanate of Oman.

³Department of mathematics, Baba Saheb Bhimrao Ambedkar University Lucknow, India.

⁴Department of Mathematics and Computer Sciences, Faculty of Arts and Sciences, Cankaya University, Ankara TR-06530, Turkey.

⁵Institute of Space Science, Magurle, Bucharest R-077125, Romania.

Abstract

In this article, we introduce a novel numerical approach for solving biological population growth models using the Vieta-Fibonacci wavelet-based collocation method (VFWM). The proposed scheme transforms the governing nonlinear differential equations into a system of algebraic equations by employing the truncated Vieta-Fibonacci wavelet, which is then solved via the Newton-Raphson method. To the best of our knowledge, we also apply the Haar wavelet method (HWM) to these models for the first time, providing a new benchmark for comparison. A comprehensive set of numerical experiments on diverse population growth models demonstrate the robustness of VFWM in handling nonlinear dynamics. The results show that VFWM consistently outperforms HWM and other existing numerical schemes, such as the Runge-Kutta-Fehlberg method and the Laplace Adomian Decomposition Method, both in terms of accuracy and computational efficiency. The convergence and error analysis further confirm the stability and reliability of the proposed technique, establishing VFWM as a powerful and efficient tool for the numerical study of biological systems.

Keywords. Vieta-Fibonacci wavelet, Vieta-Fibonacci operational matrix of integration, Collocation points, Biological model.

2010 Mathematics Subject Classification. 92D25, 65L05, 65T60, 37M15.

1. INTRODUCTION

Several researchers have developed mathematical models of population growth, offering different perspectives on real ecological phenomena. Each parameter in these models holds biological significance [30, 34]. The birth and death rates of populations across different species fluctuate periodically, particularly in the case of insect populations, where these rates vary according to seasonal changes. The Lotka-Volterra equations describe a range of ecological predator-prey models, which are inherently dynamic. Holling [17, 18] introduced the predator-prey functional response based on real ecological experiments, defining the intake rate of predator species as a function of prey density. Hollings type III functional response plays a crucial role in accurately modeling population growth within population dynamics. The differential equation governing the seasonal growth of an insect population model [13] is given as

$$y'(t) = Ky(t)\cos(\lambda t), \quad (1.1)$$

where $y(t)$ denotes the population of insects over time t , while K and λ are positive constant. Equation (1.1) describes the insect food chain, accounting for mutual interference among predators and time delays during gestation across different seasons [13]. The modified form of Equation (1.1) is given by:

$$y'(t) = Ky(t)\cos(\lambda t) - \frac{\alpha y(t)^2}{\beta + y(t)^2}, \quad (1.2)$$

Received: 15 May 2025; Accepted: 31 December 2025.

* Corresponding author. Email: nikkhannak232@gmail.com, n.khanna@squ.edu.om.

where $\frac{\alpha y(t)^2}{\beta + y(t)^2}$ represents the Holling type III functional response, where α, β are positive constants, with α denoting the maximum capture rate of insects by a predator species. By incorporating the interspecific competition term into Equation (1.2), the modified insect population growth equation [21, 23] is expressed as

$$y'(t) = Ky(t)\cos(\lambda t) - \frac{\alpha y(t)^2}{\beta + y(t)^2} - \mu y(t)^2, \quad (1.3)$$

where μ represents the coefficient of interspecific competition. The mathematical model for single-species or multi-species populations can also be defined using other well-known equations. The Lotka-Volterra model for a single species [14, 28] is given as

$$y'(t) = y(t)(b - ay(t)), \quad a > 0, b > 0, y(0) > 0, \quad (1.4)$$

where a, b are positive constants.

If the Holling type III functional response is incorporated into Equation (1.4), the modified model can be expressed as:

$$y'(t) = y(t)(b - ay(t)) - \frac{\alpha y(t)^2}{\beta + y(t)^2}, \quad (1.5)$$

where $\frac{\alpha y(t)^2}{\beta + y(t)^2}$ represents the Holling type III functional response, and α, β are positive constants. Here, α is referred to as the predation rate, while β is known as the half-saturation constant.

Various researchers have employed different methods to solve nonlinear differential equations. Some of the well-known approaches include the Homotopy Perturbation Method (HPM) [41], Homotopy Analysis Method (HAM) [43], Differential Transform Method (DTM) [42], Variational Iteration Method (VIM) [16], Adomian Decomposition Method (ADM) [11], Laplace Adomian Decomposition Method (LADM) [31, 32], Runge-Kutta-Fehlberg Method (RKFM) [31, 32], Haar Wavelet Method (HWM) [39], Legendre Wavelet Method (LWM) [36], and Genocchi Wavelet Method (GNW) [38]. These methods have been widely used to tackle nonlinear differential equations effectively.

In the past few years, a number of significant contributions have enriched the field of fractional calculus and its applications to nonlinear models. For instance, Agarwal et al. developed hybrid methods for fractional Whitham-Broer-Kaup equations [2], while Ahmad et al. studied coupled Hilfer-Hadamard fractional differential systems with nonlocal conditions [3]. Baleanu et al. proposed a fractional model for tumor-immune surveillance [6], and Ebrahimzadeh et al. introduced fractional modeling techniques for water pollution management [12]. Furthermore, Hashemi et al. [15], Nourian et al. [27], and Park et al. [29] explored novel wavelet-based discretizations and solution strategies for fractional-order differential equations. These works highlight the growing importance of fractional calculus in biological, physical, and financial systems, providing further motivation for the present study.

1.1. Plan of work. The article is organized as follows: In section 2, a comprehensive introduction to the Vieta-Fibonacci wavelet is provided, focusing on its orthonormal basis properties and the process of its construction. Additionally, the operational matrix of integration for the Vieta-Fibonacci wavelet is derived, forming the basis for function approximation and subsequent numerical implementation. Section 3 presents the theoretical framework underpinning the convergence of the proposed method. This section includes a rigorous error analysis to ensure the stability and reliability of the wavelet-based approach. The error bounds derived in this section demonstrate the method's accuracy in solving nonlinear biological models. Section 4 showcases several numerical examples to demonstrate the efficiency and precision of the proposed method. Various biological growth models, including insect population dynamics and the Lotka-Volterra models, are solved using the Vieta-Fibonacci wavelet-based collocation approach. The results obtained are compared with those derived from the Haar Wavelet Method and the existing numerical techniques, such as the Runge-Kutta-Fehlberg Method and the Laplace Adomian Decomposition Method, emphasizing the advantages of the proposed approach.

2. VIETA-FIBONACCI WAVELET: MATHEMATICAL FRAMEWORK AND METHOD

Wavelets constitute a family of functions derived from a single fundamental function, known as the mother wavelet, through transformation, dilation, and translation operations. When the dilation parameter i and translation parameter



j are continuous, the family of continuous wavelets is defined as:

$$\psi_{i,j}(x) = |i|^{-\frac{1}{2}} \psi\left(\frac{x-j}{i}\right), \quad i, j \in \mathbb{R}, \quad i \neq 0. \tag{2.1}$$

By restricting the parameters to discrete values, i.e., setting $i = a_0^{-m}$ and $j = nb_0 a_0^{-m}$, where $a_0 > 1$, $b_0 > 1$, and $n, m \in \mathbb{N}$, the corresponding discrete wavelet family is given by:

$$\psi_{n,m}(x) = |a_0|^{\frac{m}{2}} \psi(a_0^m x - nb_0). \tag{2.2}$$

Here, $\psi_{n,m}$ forms a wavelet basis for the space $L^2(\mathbb{R})$. In particular, when $a_0 = 2$ and $b_0 = 1$, the wavelet basis $\psi_{n,m}(x)$ constitutes an orthonormal basis. For more details on wavelets, one may read [10, 19, 20, 33].

In parallel, fractional-order wavelet techniques have been successfully applied to challenging problems, including delay fractional differential equation of pantograph type [15], time-fractional Black-Scholes models [27], and multi time-fractional telegraph equation of distributed order [29]. These developments emphasize the versatility of wavelet-based approaches in fractional settings, further supporting their extension to biological growth models considered here. Among various wavelet families, Vieta-Fibonacci wavelets have emerged as an effective computational tool due to their orthonormal properties and computational efficiency. Their applications in solving fractional differential equations, integrodifferential equations, and delay differential systems have been extensively explored in recent literature. This section presents an overview of recent advancements in numerical techniques based on Vieta-Fibonacci wavelets.

The theoretical foundation of Vieta-Fibonacci wavelets was introduced by Azin et al. [4], who developed an operational matrix for fractional integration and demonstrated its effectiveness in solving fractional pantograph equations. The method involved transforming the given problem into a system of algebraic equations, thereby facilitating an efficient computational approach.

Subsequent research has further extended the applicability of these wavelets. Azin et al. [5] proposed an extended framework by formulating fractional Vieta-Fibonacci wavelets for solving systems of fractional delay differential equations. This work introduced some relationships regarding fractional integration and derivative of these wavelets and applied them within the collocation method, resulting in efficient numerical approximations.

Several researchers have investigated collocation and projection methods based on Vieta-Fibonacci polynomials for various differential equations. Notable contributions include: Rahimkhani et al. (2024) [35] developed a fractal-fractional integral operator approach using Vieta-Fibonacci polynomials for solving pantograph and chaotic systems. Moumen et al. (2023) [24] introduced a Vieta-Fibonacci projection method for fractional integrodifferential equations and validated its efficiency through error analysis and computational results. Sadri et al. (2022) [37] proposed a matrix collocation method for fractional delay integro-differential equations.

Collectively, these studies establish the robustness of Vieta-Fibonacci wavelets in transforming complex differential problems into simpler algebraic forms, thereby enhancing computational efficiency.

The Vieta-Fibonacci wavelet [4] is defined on $[0,1)$ as

$$\psi_{n,m}(t) = \begin{cases} 2^{k/2} \sqrt{\frac{8}{\pi}} V_m(2^k t - n), & \text{for } \frac{n}{2^k} \leq t \leq \frac{n+1}{2^k} \\ 0, & \text{Otherwise,} \end{cases} \tag{2.3}$$

where, $m = 1, 2, \dots, M; n = 0, 1, 2, 3, \dots, 2^k - 1$ and $k \in \mathbb{N} \cup \{0\}$. $V_m(t)$ are Vieta-Fibonacci polynomials of order m , defined on $[0, 1]$. The few Vieta-Fibonacci polynomials $V_m(t)$ of order m is given as:

$$\begin{aligned} V_1(t) &= 1, \\ V_2(t) &= (-2 + 4t), \\ V_3(t) &= (3 - 16t + 16t^2), \\ V_4(t) &= (-4 + 40t - 96t^2 + 64t^3), \end{aligned}$$



$$\begin{aligned} V_5(t) &= \left(5 - 80t + 336t^2 - 512t^3 + 256t^4 \right), \\ V_6(t) &= \left(-6 + 140t - 896t^2 + 2304t^3 - 2560t^4 + 1024t^5 \right), \\ V_7(t) &= \left(7 - 224t + 2016t^2 - 7680t^3 + 14080t^4 - 12288t^5 + 4096t^6 \right). \end{aligned}$$

For $k = 0$ and $M = 6$, the few Vieta-Fibonacci wavelets are given as:

$$\begin{aligned} \psi_{0,1}(t) &= 2\sqrt{\frac{2}{\pi}}, \\ \psi_{0,2}(t) &= 2\sqrt{\frac{2}{\pi}} \left(-2 + 4t \right), \\ \psi_{0,3}(t) &= 2\sqrt{\frac{2}{\pi}} \left(3 - 16t + 16t^2 \right), \\ \psi_{0,4}(t) &= 2\sqrt{\frac{2}{\pi}} \left(-4 + 40t - 96t^2 + 64t^3 \right), \\ \psi_{0,5}(t) &= 2\sqrt{\frac{2}{\pi}} \left(5 - 80t + 336t^2 - 512t^3 + 256t^4 \right), \\ \psi_{0,6}(t) &= 2\sqrt{\frac{2}{\pi}} \left(-6 + 140t - 896t^2 + 2304t^3 - 2560t^4 + 1024t^5 \right), \\ \psi_{0,7}(t) &= 2\sqrt{\frac{2}{\pi}} \left(7 - 224t + 2016t^2 - 7680t^3 + 14080t^4 - 12288t^5 + 4096t^6 \right). \end{aligned}$$

Vieta-Fibonacci wavelets have been successfully applied across diverse scientific and engineering domains, highlighting their versatility in solving real-world problems. In 2021, Agarwal et al. [1] utilized Vieta-Fibonacci operational matrices for spectral solutions of variable-order fractional integro-differential equations, demonstrating their effectiveness in physics and engineering. Later in 2023, Nayied et al. [26] explored the numerical assessment of brain tumor growth models using Fibonacci wavelets, illustrating their potential in medical applications. Furthermore in 2024, Kumar et al. [22] applied a Fibonacci wavelet-based collocation method for modeling dengue fever transmission, proving its utility in epidemiological studies. These applications underscore the growing interdisciplinary significance of Vieta-Fibonacci wavelet-based numerical methods, making them a promising tool for both theoretical and applied research.

2.1. Vieta-Fibonacci operational matrix of integration. Now, we construct the operational matrix of integration of Vieta-Fibonacci wavelet for $k = 0$, $M = 6$. Let

$$\psi(t) = \left(\psi_{0,1}(t), \psi_{0,2}(t), \psi_{0,3}(t), \psi_{0,4}(t), \psi_{0,5}(t), \psi_{0,6}(t) \right)^T,$$

be the Vieta-Fibonacci wavelets basis. Note that the integral of $\psi(t)$ with respect to t can be defined as follows:

$$\begin{aligned} p_{0,1}(x) &= \int_0^t \psi_{0,1}(t) dt = \int_0^t 2\sqrt{\frac{2}{\pi}} dt = 2\sqrt{\frac{2}{\pi}} t \\ &= \frac{1}{2}\psi_{0,1} + \frac{1}{4}\psi_{0,2} + 0\psi_{0,3} + 0\psi_{0,4} + 0\psi_{0,5} + 0\psi_{0,6} \\ &= \left[\frac{1}{2}, \frac{1}{4}, 0, 0, 0, 0 \right] \psi(t), \end{aligned}$$



$$\begin{aligned}
 p_{0,2}(x) &= \int_0^t \psi_{0,2}(t)dt = \int_0^t 2\sqrt{\frac{2}{\pi}}(-2 + 4t)dt = 2\sqrt{\frac{2}{\pi}}(-2t + 2t^2) \\
 &= \frac{-3}{8}\psi_{0,1} + 0\psi_{0,2} + \frac{1}{8}\psi_{0,3} + 0\psi_{0,4} + 0\psi_{0,5} + 0\psi_{0,6} \\
 &= \left[\frac{-3}{8}, 0, \frac{1}{8}, 0, 0, 0\right]\psi(t), \\
 p_{0,3}(x) &= \int_0^t \psi_{0,3}(t)dt = \int_0^t 2\sqrt{\frac{2}{\pi}}(3 - 16t + 16t^2)dt = 2\sqrt{\frac{2}{\pi}}\left(3t - 8t^2 + \frac{16}{3}t^3\right) \\
 &= \frac{1}{6}\psi_{0,1} - \frac{1}{12}\psi_{0,2} + 0\psi_{0,3} + \frac{1}{12}\psi_{0,4} + 0\psi_{0,5} + 0\psi_{0,6} \\
 &= \left[\frac{1}{6}, \frac{-1}{12}, 0, \frac{1}{12}, 0, 0\right]\psi(t), \\
 p_{0,4}(x) &= \int_0^t \psi_{0,4}(t)dt = \int_0^t 2\sqrt{\frac{2}{\pi}}(-4 + 40t - 96t^2 + 64t^3)dt = 2\sqrt{\frac{2}{\pi}}(-4t + 20t^2 - 32t^3 + 16t^4) \\
 &= \frac{1}{8}\psi_{0,1} + 0\psi_{0,2} - \frac{1}{16}\psi_{0,3} + 0\psi_{0,4} + \frac{1}{16}\psi_{0,5} + 0\psi_{0,6} \\
 &= \left[\frac{1}{8}, 0, \frac{-1}{16}, 0, \frac{1}{16}, 0\right]\psi(t), \\
 p_{0,5}(x) &= \int_0^t \psi_{0,5}(t)dt = \int_0^t 2\sqrt{\frac{2}{\pi}}(5 - 80t + 336t^2 - 512t^3 + 256t^4)dt \\
 &= 2\sqrt{\frac{2}{\pi}}\left(5t - 40t^2 + 112t^3 - 123t^4 + \frac{256}{5}t^5\right) \\
 &= \frac{1}{10}\psi_{0,1} + 0\psi_{0,2} + 0\psi_{0,3} - \frac{1}{20}\psi_{0,4} + 0\psi_{0,5} + \frac{1}{20}\psi_{0,6} \\
 &= \left[\frac{1}{10}, 0, 0, \frac{-1}{20}, 0, \frac{1}{20}\right]\psi(t), \\
 p_{0,6}(t) &= \int_0^t \psi_{0,6}(t)dt = \int_0^t 2\sqrt{\frac{2}{\pi}}(-6 + 140t - 896t^2 + 2304t^3 - 2560t^4 + 1024t^5)dt \\
 &= 2\sqrt{\frac{2}{\pi}}\left(-6t + 70t^2 - \frac{896}{3}t^3 + 576t^4 - 512t^5 + \frac{512}{3}t^6\right) \\
 &= \frac{-1}{12}\psi_{0,1} + 0\psi_{0,2} + 0\psi_{0,3} + 0\psi_{0,4} - \frac{1}{24}\psi_{0,5} + 0\psi_{0,6} + \frac{1}{24}\psi_{0,7} \\
 &= \left[\frac{-1}{12}, 0, 0, 0, \frac{-1}{24}, 0\right]\psi(t) + \frac{1}{24}\psi_{0,7}.
 \end{aligned}$$

Hence,

$$\int_0^t \psi(t)dt = P_{6 \times 6}\psi(x) + \bar{\psi}_6(t), \tag{2.4}$$



where $P_{6 \times 6}$ is a operational matrix of integration of order 6, defined as:

$$P_{6 \times 6} = \begin{pmatrix} \frac{1}{2} & \frac{1}{4} & 0 & 0 & 0 & 0 \\ \frac{3}{8} & 0 & \frac{1}{8} & 0 & 0 & 0 \\ \frac{1}{6} & \frac{-1}{12} & 0 & \frac{1}{12} & 0 & 0 \\ \frac{1}{8} & 0 & \frac{-1}{16} & 0 & \frac{1}{16} & 0 \\ \frac{1}{10} & 0 & 0 & \frac{-1}{20} & 0 & \frac{1}{20} \\ \frac{1}{12} & 0 & 0 & 0 & \frac{-1}{24} & 0 \end{pmatrix}, \quad (2.5)$$

and $\bar{\psi}_6(t)$ is defined as:

$$\bar{\psi}_6(t) = \begin{pmatrix} 0 \\ 0 \\ 0 \\ 0 \\ 0 \\ \frac{1}{24} \psi_{0,7}(t) \end{pmatrix}. \quad (2.6)$$

2.2. Function approximation. Every continuous function $g(t)$ defined on $L^2([0, 1])$, can be expressed as [25]:

$$g(t) = \sum_{i=0}^{\infty} \sum_{j=1}^{\infty} c_{i,j} \psi_{i,j}(t), \quad (2.7)$$

where $c_{i,j} = \int_0^1 g(t) \psi_{i,j}(x) dt$. If the above infinite series is truncated up to finite number of terms, it is expressed as

$$g(t) = \sum_{i=0}^{2^k-1} \sum_{i=1}^M c_{i,j} \psi_{i,j}(t) = C^T \psi(t), \quad (2.8)$$

where the C is matrix of unknown vectors $c_{i,j}$ and $\psi(t)$ is a matrix of wavelet basis, of order $(2^k - 1) \times M$, expressed as:

$$C = [c_{0,1}, c_{0,2}, \dots, c_{0M}, c_{1,1}, \dots, c_{1,M}, \dots, c_{2^k-1,1}, \dots, c_{2^k-1,M}]^T,$$

$$\psi(t) = [\psi_{0,1}(t), \psi_{0,2}(t), \dots, \psi_{0,M}(t), \psi_{1,1}(t), \dots, \psi_{1,M}(t) \dots, \psi_{2^k-1,1}(t), \dots, \psi_{2^k-1,M}(t)]^T.$$

2.3. Methodology. Let us consider the equation $y'(t) = K y(t) \cos(\lambda t)$ with boundary conditions $y(0) = a$. For $k = 0$, let

$$y'(t) = \sum_{i=1}^M c_{0,i} \psi_{0,i}(t) = C^T \psi(t). \quad (2.9)$$

Then

$$y(t) = \sum_{i=1}^M c_{0,i} p_{1,i}(t) + y(a) = C^T P \psi(t) + a. \quad (2.10)$$

Therefore, the equation becomes

$$C^T \psi(t) = K (C^T P \psi(t) + a) \cos(\lambda t). \quad (2.11)$$

The collocation of Equation (2.11) is performed by taking

$$t = t_i, \quad t_i = \frac{2l-1}{2N}, \quad l = 1, 2, 3, \dots, N.$$

This procedure yields a system of N nonlinear equations. By solving these equations using the Newton-Raphson method implemented in *Mathematica*, the values of the unknown vectors $c_{i,j}$ are obtained. Substituting these vectors



into Equation (2.10) provides the Vieta-Fibonacci wavelet-based approximate solution for the insect population growth model.

3. CONVERGENCE ANALYSIS

A critical aspect of recent research on Vieta-Fibonacci-based methods is the rigorous analysis of their error bounds and convergence properties. Extensive studies have established the reliability and accuracy of these methods. Azin et al. [5] derived an upper error bound for approximation with the fractional Vieta-Fibonacci wavelets, confirming their high accuracy. Moumen et al. [24] conducted a comprehensive convergence analysis of their novel Vieta-Fibonacci projection method, demonstrating its robustness for practical applications. Sadri et al. [37] applied Krasnoselskii's fixed-point theorem to establish the uniqueness of solutions obtained via the Vieta-Fibonacci collocation method. These theoretical validations further affirm the computational efficiency and reliability of Vieta-Fibonacci wavelet-based techniques in solving complex mathematical models.

As shown in [40], a square-integrable function $f(x)$ with a bounded second derivative on $[0, 1]$ can be uniformly approximated by an infinite series of Vieta-Fibonacci wavelets, with coefficients bounded by a specific expression. We recall this result below.

Theorem 3.1. *Let $f \in L^2(\mathbb{R})$ be a function defined on $[0, 1]$ with $|f''(x)| \leq B$. Then $f(x)$ can be written as the infinite sum of the Vieta-Fibonacci wavelets $\psi_{n,m}(x)$, and the series converges uniformly to the function $f(x)$, that is*

$$f(x) = \sum_{n=0}^{\infty} \sum_{m=1}^{\infty} a_{n,m} \psi_{n,m}(x),$$

where

$$a_{n,m} \leq \frac{3}{2} \sqrt{\frac{\pi}{8}} \frac{B}{(1+n)^2(m-1)^2(m-2)^2}, \quad m \geq 2, n \geq 0.$$

In the next result, we recall the error bound established in [40] for approximating $f(x)$ using a truncated Vieta-Fibonacci wavelet series, with the error decreasing as more terms are included, and an explicit formula for the error is given.

Theorem 3.2. *Let $f(x)$ be a continuous function defined in $[0, 1]$ such that its second derivative is bounded by some constant B . Then, the error bound will be*

$$|\sigma_{n,M}| < \frac{3B}{2} \sqrt{\frac{\pi}{8}} \left(\sum_{n=0}^{\infty} \sum_{m=M+1}^{\infty} \left(\frac{1}{(1+n)^2(m-1)^2(m-2)^2} \right)^2 + \sum_{n=2^k}^{\infty} \sum_{m=1}^{\infty} \left(\frac{1}{(1+n)^2(m-1)^2(m-2)^2} \right)^2 \right)^{\frac{1}{2}},$$

where

$$\sigma_{n,M}^2 = \int_0^1 \left(f(x) - \sum_{n=0}^{2^k-1} \sum_{m=1}^M a_{n,m} \psi_{n,m}(x) \right)^2 w_n(x) dx.$$

4. NUMERICAL EXAMPLES

In this section, we present a series of numerical examples to illustrate the efficiency and accuracy of the proposed Vieta-Fibonacci wavelet-based collocation method (VFWM). The selected examples cover different biological population growth models, demonstrating the robustness of our approach in handling nonlinear differential equations. In addition to applying VFWM, we also solve these problems using the Haar wavelet method (HWM), which, to the best of our knowledge, has not previously been employed for such models. For obtaining the solutions by HWM, the number of collocation points is taken as $N = 16$. The results obtained from VFWM are systematically compared with those from HWM and other existing numerical techniques, highlighting the superior accuracy and computational efficiency of the proposed scheme. For consistency, the absolute error associated with the Vieta-Fibonacci wavelet-based collocation method (VFWM) is formally defined and denoted as follows:

$$eVFWM = \max |y(x_i) - y_{\text{approx}}(x_i)|,$$



TABLE 1. Numerical comparison when $M = 10$ and $k = 0$.

x	Exact Solution	Solution by RKFM [31]	Solution by LADM[31]	Solution by HWM	Solution by VFWM
0.0	1000.0000000	1000.0000000	1000.0000000	1000.0000000	1000.0000000
0.1	1217.41082460	1217.4447223	1216.07381402	1219.11069192	1217.41623953
0.2	1453.82165516	1453.8275070	1444.17894316	1454.66301301	1453.82819871
0.3	1673.69911337	1673.6084290	1647.56834151	1674.20961535	1673.70663908
0.4	1832.09731230	1831.8125036	1788.52160650	1830.02494694	1832.10554963
0.5	1890.08116457	1889.5159617	1838.84276708	1890.08116457	1890.08966292
0.6	1832.09731230	1831.2908389	1788.12230677	1830.02494694	1832.10554963
0.7	1673.69911337	1672.7809816	1646.85165910	1674.20961539	1673.70663908
0.8	1453.82165516	1452.9182247	1443.28432644	1454.66301301	1453.82819871
0.9	1217.41082460	1216.5807034	1215.15811427	1219.11069192	1217.41623953
1	0999.19568760	0999.26049050	0999.19564898	1000.00000000	1000.00000000

where $y(x_i)$ denotes the analytical solution and $y_{\text{approx}}(x_i)$ represents the Vieta-Fibonacci wavelet-based solution at the collocation point x_i . Similar notation is adopted to define the absolute error for the other schemes.

Example 4.1. Consider the insect population growth model $y'(t) = Ky(t)\cos(\lambda t)$ with $y(0) = 1000$ and constant term $K = 2, \lambda = \pi$.

For $k = 0$, let

$$y'(t) = \sum_{i=1}^M c_{0,i} \psi_{0,i}(t) = A^T \psi(t). \quad (4.1)$$

Then

$$y(t) = \sum_{i=1}^M c_{0,i} p_{1,i}(t) + y(0) = A^T P \psi(t) + 1000. \quad (4.2)$$

Therefore, the equation becomes

$$A^T \psi(t) = K(A^T P \psi(t) + 1000) \cos(\lambda t). \quad (4.3)$$

Now, on collocating the above equation by $t_i = \frac{2l-1}{2N}$, $l = 1, 2, 3, 4, \dots, N-1$, we obtain N set of equations with N unknown vectors which is then solved by the Newton-Raphson method.

The comparative analysis of the graphical representations obtained using VFWM, HWM, RKFM [31], and LADM [31] is presented in Table 1. The corresponding absolute errors computed by VFWM and HWM are evaluated against those reported for RKFM and LADM in [31], detailed results are provided in Table 2. Furthermore, Figure 1 depicts the graphical representation of the results for Example 4.1, while Figure 2 illustrates a comparative assessment of the absolute errors across the different methods. As observed from Table 2, VFWM requires less CPU time and exhibits higher efficiency, producing results with superior accuracy compared to the other approaches.

Example 4.2. Consider the modified insect population growth model

$$y'(t) = Ky(t)\cos(\lambda t) - \frac{\alpha y(t)^2}{\beta + y(t)^2}, \quad y(0) = 100.$$

The constant parameters are set as $K = 2, \lambda = \pi, \alpha = 0.5$, and $\beta = 0.03$. The given equation is then solved using the proposed method, as described in Example 4.1. Table 3 presents the exact solution along with the numerical solutions obtained using VFWM, HWM, and the methods reported in [31]. A comparison of the absolute errors is provided in Table 4, where the performance of VFWM and HWM is evaluated against LADM [31] and RKFM [31]. Table 4 also reports the CPU time required by the proposed method, clearly showing that VFWM achieves greater computational



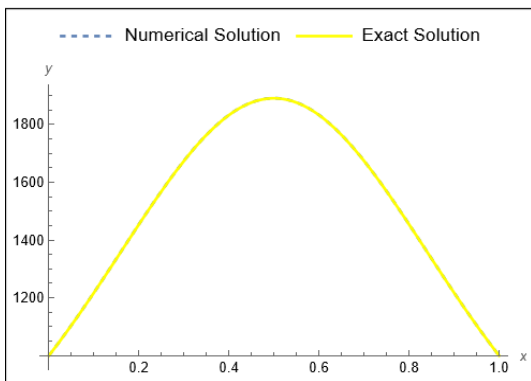


FIGURE 1. Comparison between the exact solution and the solution obtained by VFWM.

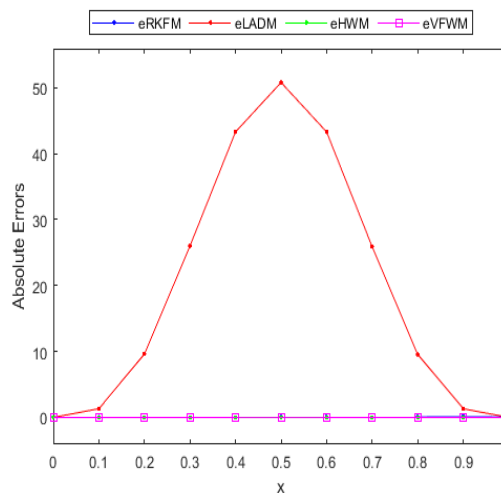


FIGURE 2. Comparison of absolute errors.

TABLE 2. Comparison of absolute errors.

x	eRKFM [31]	eLADM [31]	eHWM	eVFWM	CPU Time (in Sec.)
0.0	0.0 e - 00	e + 00	0.0000 e - 00	0.0 e - 00	0.15625
0.1	3.71 e - 02	1.33 e + 00	1.69986 e + 00	5.41493 e - 03	0.18750
0.2	3.54 e - 02	9.61 e + 00	8.41358 e - 01	6.54355 e - 03	0.14062
0.3	1.87 e - 02	2.60 e + 01	5.10502 e - 01	7.52571 e - 03	0.07812
0.4	2.07 e - 02	4.33 e + 01	2.07237 e + 00	8.23733 e - 03	0.10937
0.5	8.10 e - 02	5.08 e + 01	2.98387 e + 00	8.49835 e - 03	0.10937
0.6	8.68 e - 02	4.33 e + 01	2.07237 e + 00	8.23733 e - 03	0.12500
0.7	1.72 e - 02	2.59 e + 01	5.10502 e - 01	7.52571 e - 03	0.12500
0.8	7.25 e - 02	9.56 e + 00	8.41358 e - 01	6.54355 e - 03	0.10937
0.9	1.04 e - 01	1.32 e + 0	1.69987 e + 00	5.41493 e - 03	0.10937
1	6.48 e - 02	3.86 e - 05	0.0000 e - 00	3.51406 e - 10	0.12500

efficiency than the other schemes. Furthermore, Figures 3 and 4 present graphical representations of the comparative analysis of the approximate solutions and absolute errors, respectively, for Example 4.2.

Example 4.3. Consider the modified insect population growth model

$$y'(t) = Ky(t)\cos(\lambda t) - \frac{\alpha y(t)^2}{\beta + y(t)^2} - \mu y(t)^2, \quad y(0) = 100.$$

The constant parameters are set as $K = 2$, $\lambda = \pi$, $\alpha = 0.5$, $\beta = 0.03$, and $\mu = 0.00001$. The given equation is solved using the proposed method, as described in Example 4.1. Table 5 presents the exact solution along with the numerical solutions obtained using VFWM, HWM, and the methods reported in [31]. In Table 6, the absolute errors produced by VFWM are compared with those of LADM [31], RKFM [31], and HWM. Table 6 also highlights that the proposed scheme requires significantly less CPU time and exhibits a better rate of convergence. Furthermore, Figures 5 and 6 present graphical representations of the comparative analysis of the approximate solutions and absolute errors, respectively, for Example 4.3.

Example 4.4. Consider the Lotka-Volterra insect population growth model

$$y'(t) = y(t)(b - ay(t)), \quad y(0) = 0.1.$$



TABLE 3. Numerical comparison when $M = 10$ and $k = 0$.

x	Exact Solution	Solution by RKFM [31]	Solution by LADM[31]	Solution by HWM	Solution by VFWM
0.0	100.0000000	100.0000000	100.0000000	100.0000000	100.0000000
0.1	121.68557411	121.108106	121.5572303	121.85527993	121.71112871
0.2	145.25872028	143.9584501	144.3172756	145.34534905	145.29058960
0.3	167.16677455	165.1252092	164.6053933	167.22827569	167.21114888
0.4	182.92083874	180.3198596	178.6494928	182.73989950	182.98382247
0.5	188.63838966	185.8501193	183.6299329	188.98437003	188.72454396
0.6	182.7773689	180.2468100	178.5057434	182.64227699	182.88587071
0.7	166.9030599	164.9840041	164.3260955	167.04386317	167.02649760
0.8	144.9109052	143.7574377	143.9164278	145.09218769	145.03726185
0.9	121.2890397	120.8566363	121.0506779	121.55195822	121.40758757
1	99.57968623	99.70572240	99.40133120	100.00000000	99.65988697

TABLE 4. Comparison of absolute errors for $M=14$, $k=0$.

x	eRKFM [31]	eLADM [31]	eHWM	eVFWM	CPU Time (in Sec.)
0.0	0.00 e + 00	0.00 e + 00	0.00000 e - 00	0.00000 e - 00	0.40625
0.1	5.77 e - 01	1.28 e - 01	1.69407 e - 01	5.37196 e - 04	0.45312
0.2	1.30 e - 01	9.41 e - 01	8.3695 e - 02	6.47468 e - 04	0.46875
0.3	2.04 e + 00	2.56 e + 00	5.06015 e - 02	7.49442 e - 04	0.45312
0.4	2.60 e + 00	4.27 e + 00	2.07307 e - 01	8.27197 e - 04	0.48437
0.5	2.79 e + 00	5.01 e + 00	2.97611 e - 01	8.51092 e - 04	0.42187
0.6	2.53 e + 00	4.27 e + 00	2.06981 e - 01	8.24347 e - 04	0.45312
0.7	1.92 e + 00	2.58 e + 00	5.08400 e - 02	7.49057 e - 04	0.43750
0.8	1.15 e + 00	9.94 e - 01	8.38561 e - 02	6.42786 e - 04	0.50000
0.9	4.32 e - 01	2.38 e - 01	1.69618 e - 01	5.2439 e - 04	0.42187
1	1.26 e - 01	1.78 e - 01	1.340041 e - 01	2.10133 e - 06	0.48437

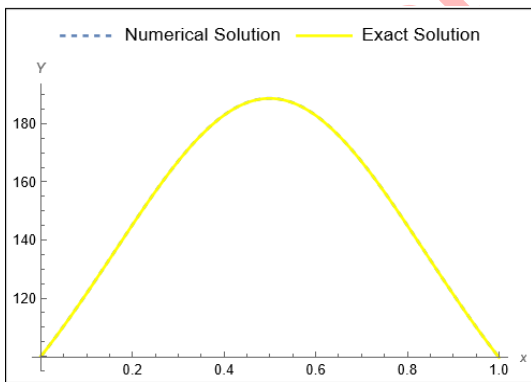


FIGURE 3. Comparison between the exact solution and the solution obtained by VFWM.

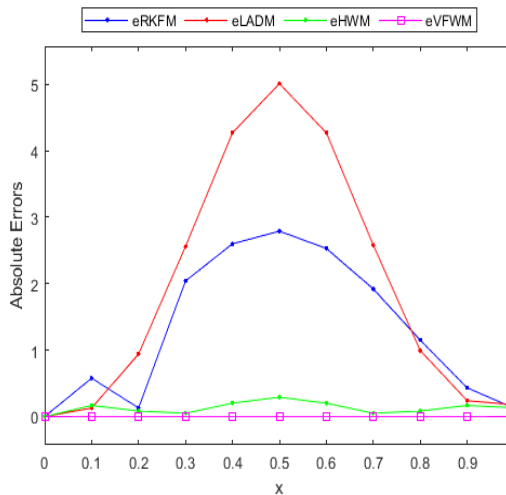


FIGURE 4. Comparison of absolute errors.



TABLE 5. Numerical comparison when $M = 10$ and $k = 0$.

x	Exact Solution	Solution by RKFM [31]	Solution by LADM[31]	Solution by HW	Solution by VFWM
0.0	100.000000	100.0000000	1000.0000000	100.0000000	100.0000000
0.1	121.672100	121.679140	121.5472313	121.84132464	121.67294584
0.2	145.223200	145.251020	144.2972796	145.30937319	145.22684226
0.3	167.099800	167.157910	164.5754023	167.16069648	167.11144417
0.4	182.8154000	182.911160	178.6095088	182.63398908	182.84258711
0.5	188.4945000	188.628430	183.5799579	188.83985141	188.54362916
0.6	182.6038000	182.767730	178.4457794	182.46880830	182.67643057
0.7	166.715300	166.894240	164.2561445	166.85592846	166.80586366
0.8	144.725200	144.903240	143.8364918	144.90625960	144.82313468
0.9	121.117500	121.282630	120.9607589	121.38004721	121.21112146
1	099.427800	099.574430	099.3014312	100.00000000	099.50792154

TABLE 6. Comparison of absolute errors.

x	eRKFM [31]	eLADM [31]	eHWM	eVFWM	CPU Time (in Sec.)
0.0	0.00 e + 00	0.00 e + 00	0.00000 e - 00	0.00000 e - 00	0.53125
0.1	7.04 e - 03	1.25 e - 01	1.68906 e - 01	5.30517 e - 04	0.56250
0.2	2.77 e - 02	9.26 e - 01	8.31701 e - 02	6.39219 e - 04	0.56250
0.3	4.18 e - 02	2.52 e + 00	4.99921 e - 02	7.3974 e - 04	0.45312
0.4	7.63 e - 02	4.21 e + 00	2.07782 e - 01	8.16157 e - 04	0.56250
0.5	1.15 e - 01	4.91 e + 00	2.97062 e - 01	8.39534 e - 04	0.48437
0.6	1.64 e - 01	4.16 e + 00	2.0681 e - 01	8.12692 e - 04	0.64062
0.7	1.79 e - 01	2.46 e + 00	5.0803 e - 02	7.38181 e - 04	0.53125
0.8	1.78 e - 01	8.89 e - 01	8.37581 e - 02	6.33162 e - 04	0.56250
0.9	1.65 e - 01	1.57 e - 01	1.69442 e - 01	5.15839 e - 04	0.48437
1	1.47 e - 01	1.26 e - 01	0.00000 e - 00	1.36601 e - 05	0.50000

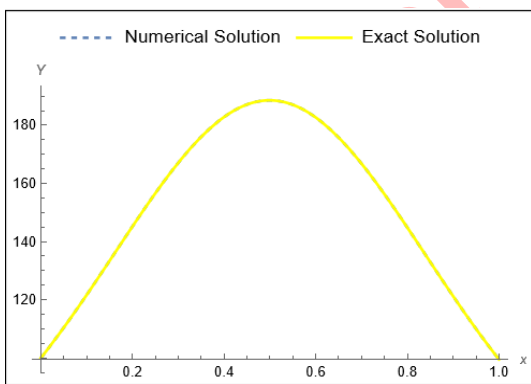


FIGURE 5. Comparison between the exact solution and the solution obtained by VFWM.

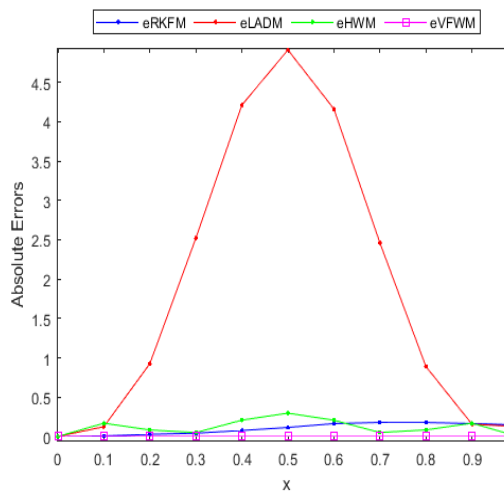


FIGURE 6. Comparison of absolute errors.



TABLE 7. Numerical comparison when $M = 10$ and $k = 0$.

x	Exact Sol.	Solution by DTM [8]	Solution by LADM[31]	Solution by DJM[7]	Solution by VIM[9]	Solution by HWM	Solution by VFWM
0.0	0.10000000	0.10000000	0.10000000	0.10000000	0.10000000	0.10000000	0.10000000
0.1	0.10713679		0.10714000			0.10714985	0.10713678
0.2	0.11453291	0.1145329	0.11456000	0.1145329	0.1145545	0.114541841	0.11453290
0.3	0.12216385		0.12226000			0.12217295	0.12216385
0.4	0.13000114	0.1300004	0.13024000	0.1300011	0.1302590	0.13001260	0.13000113
0.5	0.13801261		0.13850000			0.138016768	0.13801261
0.6	0.14616290	0.1461546	0.14704000	0.1461627	0.1474445	0.146172636	0.14616289
0.7	0.15441399		0.15586000			0.15442140	0.15441399
0.8	0.16272591	0.1626790	0.16496000	0.1627256	0.1671263	0.16273307	0.16272591
0.9	0.17105750		0.17434000			0.17106344	0.171057495
1	0.17936718	0.1791887	0.17936718	0.1793669	0.1915249	0.10000000	0.17936717

TABLE 8. Comparison of absolute errors.

x	eDTM [8]	eDJM[7]	eLADM [31]	eVIM[9]	eHWM	eVFWM	CPU Time
0.0	0.0	0.0 e - 00	0.0 e + 00	0.0	0.00000 e - 00	0.0 e - 00	0.29687
0.1	-	-	0.0 e - 05	-	1.30639 e - 05	2.99 e - 09	0.31250
0.2	1.00 e - 08	3.8 e - 09	0.0 e - 05	2.1 e - 05	8.94569 e - 06	9.31 e - 09	0.31250
0.3	-	-	9.61 e - 05	-	9.10823 e - 06	1.51 e - 09	0.26562
0.4	7.4 e - 07	4.0 e - 08	2.39 e - 04	2.5 e - 04	1.14630 e - 05	1.47 e - 09	0.26562
0.5	-	-	4.87 e - 04	-	4.14985 e - 06	6.45e - 09	0.29687
0.6	8.3 e - 06	6.4 e - 07	8.77 e - 04	1.2 e - 03	9.72383 e - 06	1.38 e - 08	0.31250
0.7	-	-	1.45 e - 03	-	7.40608 e - 06	1.02 e - 08	0.31250
0.8	4.6 e - 05	3.2 e - 07	2.33 e - 03	4.4 e - 03	7.15191 e - 06	8.19 e - 09	0.29687
0.9	-	-	3.28 e - 03	-	5.94218 e - 06	7.70 e - 09	0.28125
1	1.7 e - 04	2.8 e - 07	4.63 e - 03	1.2 e - 02	7.93672 e - 02	7.77 e - 09	0.29687

The constant parameters are set as $a = 1$ and $b = 3$. The given equation is solved using the proposed method, as described in Example 4.1. Table 7 presents the exact solution alongside the numerical solutions obtained using VFWM, HWM, as well as DTM [8], VIM [9], LADM [31], and the Daftardar-Gejji and Jafari Method (DJM) [7]. In Table 8, the absolute errors of the proposed scheme are compared with those of DTM [8], VIM [9], LADM [31], DJM [7], and HWM. From Table 8, it can be seen that the proposed scheme outclasses the other methods, requiring significantly less CPU time. Furthermore, Figures 7 and 8 provide graphical representations of the comparative analysis of the approximate solutions and absolute errors, respectively, for Example 4.4.

Example 4.5. Consider the modified single species Lotka-Volterra insect population growth model

$$y'(t) = y(t)(b - ay(t)) - \frac{\alpha y(t)^2}{\beta + y(t)^2}, \quad y(0) = 0.1.$$

The constant parameters are set as $a = 1$, $b = 3$, $\alpha = 0.5$, and $\beta = 1$. The given equation is solved using the proposed method, as described in Example 4.1. Table 9 presents the exact solution alongside the numerical solutions obtained using VFWM, HWM, and the methods reported in [31]. In Table 10, the absolute errors of the proposed method are compared with those of LADM [31], RKFM [31], and HWM. The CPU time required by the proposed scheme, as reported in Table 10, is considerably lower, demonstrating that the proposed scheme is more reliable and efficient. Furthermore, Figures 9 and 10 provide graphical representations of the comparative analysis of the approximate solutions and absolute errors, respectively, for Example 4.5.



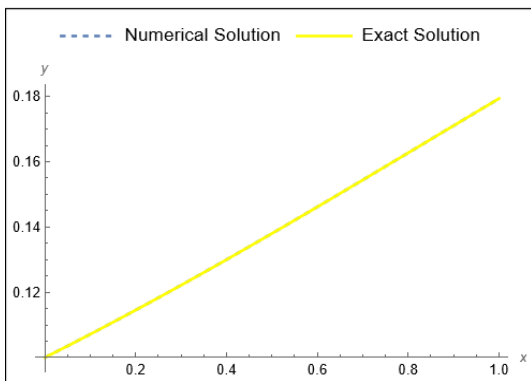


FIGURE 7. Comparison between the exact solution and the solution obtained by VFWM.

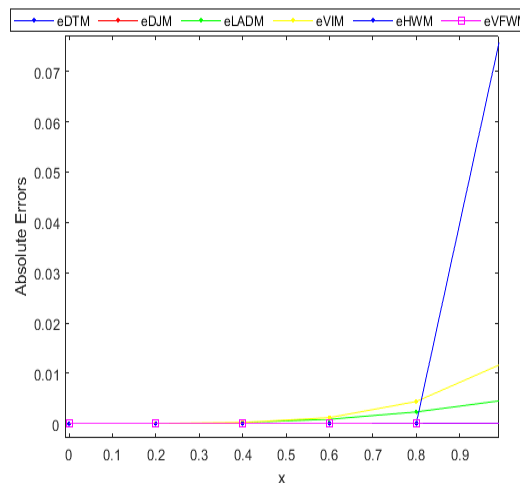


FIGURE 8. Comparison of absolute errors.

TABLE 9. Numerical comparison when $M = 10$ and $k = 0$.

x	Exact Solution	Solution by RKFM [31]	Solution by LADM[31]	Solution by HWM	Solution by VFWM
0.0	0.10000000	0.10000000	0.10000000	0.1000000000	0.1000000000
0.1	0.1065991220	0.1065991220	0.1065049505	0.10660787	0.1065991220
0.2	0.1133693593	0.1133693590	0.1130099010	0.11337504	0.1133693589
0.3	0.1202826611	0.1202826611	0.1195148515	0.12028827	0.1202826611
0.4	0.1273083819	0.1273083815	0.1260198020	0.12731466	0.1273083815 xxx
0.5	0.1344137893	0.1344137893	0.1325247525	0.13441700	0.1344137893
0.6	0.1415646647	0.1415646643	0.1390297030	0.14156902	0.1415646643
0.7	0.1487259514	0.1487259514	0.1455346535	0.14872941	0.1487259514
0.8	0.1558624471	0.1558624468	0.1520396040	0.15586564	0.1558624468
0.9	0.1629394898	0.1629394898	0.1585445545	0.16294052	0.1629394898
1	0.1699236292	0.1699236290	0.1650495050	0.1	0.1699236289

TABLE 10. Comparison of absolute errors.

x	eRKFM [31]	eLADM [31]	eHWM	eVFWM	CPU Time (in Sec.)
0.0	0.0 e - 00	0.0 e - 00	0.00000 e - 00	0.0 e - 00	0.59375
0.1	0.0 e - 00	0.0 e - 05	8.7495 e - 06	0.0 e - 00	0.60937
0.2	3.0 e - 10	0.0 e - 04	5.69303 e - 06	0.0 e - 09	0.60937
0.3	0.0 e - 00	9.61 e - 04	5.61215 e - 06	0.0 e - 00	0.60937
0.4	4.0 e - 10	2.39 e - 03	6.26675 e - 06	0.0 e - 10	0.59375
0.5	0.0 e - 00	4.87 e - 03	3.1998 e - 06	0.0e - 00	0.64062
0.6	4.0 e - 10	8.77 e - 03	4.34204 e - 06	2.1 e - 10	0.53125
0.7	0.0 e - 00	1.45 e - 03	3.44221 e - 06	0.0 e - 00	0.54687
0.8	3.0 e - 10	2.33 e - 03	3.18626 e - 06	1.36 e - 10	0.64062
0.9	0.0 e - 00	3.28 e - 03	1.01667 e - 06	0.0 e - 00	0.59375
1	2.0 e - 10	4.63 e - 03	6.99236 e - 02	1.5 e - 09	0.62500



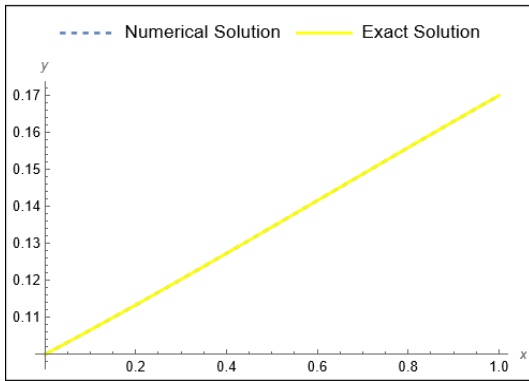


FIGURE 9. Evaluation between the exact solution and the solution obtained by VFWM.

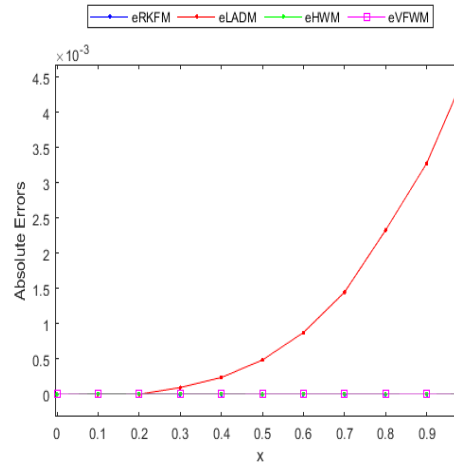


FIGURE 10. Comparison of absolute errors.

CONCLUSION

The numerical examples presented in this study confirm that the Vieta-Fibonacci wavelet-based collocation method (VFWM) is a highly efficient and accurate framework for solving nonlinear biological growth models. By reducing the original differential equations to algebraic systems, VFWM provides precise approximations with minimal computational cost. In addition, this work reports, for the first time, the application of the Haar wavelet method (HWM) to such biological models. The inclusion of HWM not only broadens the methodological landscape but also provides a meaningful baseline for comparison.

The comparative analysis across VFWM, HWM, and established techniques, including the Runge-Kutta-Fehlberg method and the Laplace Adomian Decomposition Method, clearly highlights the superior performance of VFWM in terms of both accuracy and computational efficiency. The results also demonstrate that VFWM achieves higher rates of convergence and requires significantly less CPU time than its counterparts.

Overall, the combination of rigorous convergence analysis and extensive numerical validation underlines the robustness and applicability of VFWM to a broad class of population dynamics models. Future extensions of this work may include applications to multi-species interactions, stochastic systems, and fractional-order biological models, further showcasing the versatility of the approach.

ACKNOWLEDGMENT

The authors thank the referee for insightful feedback and constructive suggestions.

DATA AVAILABILITY

No data were used to support this study.

CONFLICTS OF INTEREST

The authors declare that they have no conflicts of interest.

REFERENCES

- [1] P. Agarwal, A. A. E. El-Sayed, and J. Tariboon, *Vieta-Fibonacci operational matrices for spectral solutions of variable-order fractional integro-differential equations*, *J. Comput. Appl. Math.*, 382 (2021), Paper No. 113063, 11.



- [2] G. Agarwal, L. K. Yadav, K. S. Nisar, M. M. Alqarni, and E. E. Mahmoud, *A hybrid method for the analytical solution of time fractional Whitham-Broer-Kaup equations*, Appl. Comput. Math., 23(1) (2024), 3–17.
- [3] B. Ahmad, A. Alsaedi, S. K. Ntouyas, and F. M. Alotaibi, *A coupled Hilfer-Hadamard fractional differential system with nonlocal fractional integral boundary conditions*, TWMS J. Pure Appl. Math., 15(1) (2024), 95–114.
- [4] H. Azin, M. H. Heydari and F. Mohammadi, *Vieta-Fibonacci wavelets: Application in solving fractional pantograph equations*, Math. Methods Appl. Sci., 45 (2022), 411–422.
- [5] H. Azin, M. H. Heydari, O. Baghani, and F. Mohammadi, *Fractional Vieta-Fibonacci wavelets: application for systems of fractional delay differential equations*, Phys. Scr., 98(9) (2023), 095242.
- [6] D. Baleanu, A. Jajarmi, S. S. Sajjadi, and D. Mozyrska, *A new fractional model and optimal control of a tumor-immune surveillance with non-singular derivative operator*, Chaos, 29(8) (2019), 083127, 15.
- [7] B. Batiha, F. Ghanim, O. Alayed, R. Hatamleh, A. S. Heilat, H. Zureigat, and O. Bazighifan, *Solving Multispecies Lotka-Volterra Equations by the Daftardar-Gejji and Jafari Method*, Int. J. Math. Math. Sci., 2022 (2022), 1–7.
- [8] B. Batiha, *Comparison of numerical methods for solving one species Lotka-Volterra equation*, An. Univ. Oradea Fasc. Mat., 19(1) (2012), 243–253.
- [9] B. Batiha, M. S. M. Noorani, and I. Hashim, *Variational iteration method for solving multispecies Lotka-Volterra equations*, Comput. Math. Appl., 54(7-8) (2007), 903–909.
- [10] A. Boggess and F. J. Narcowich, *A first course in wavelets with Fourier analysis*, second edition, Wiley, Hoboken, NJ, 2009.
- [11] A. Ebaid, *A new analytical and numerical treatment for singular two-point boundary value problems via the Adomian decomposition method*, J. Comput. Appl. Math., 235(8) (2011), 1914–1924.
- [12] A. Ebrahimzadeh, A. Jajarmi, and D. Baleanu, *Enhancing water pollution management through a comprehensive fractional modeling framework and optimal control techniques*, J. Nonlinear Math. Phys., 31(1) (2024), Paper No. 48, 24.
- [13] L. H. Erbe, H. I. Freedman and V. Sree Hari Rao, *Three-species food-chain models with mutual interference and time delays*, Math. Biosci., 80(1) (1986), 57–80.
- [14] M. Fan, K. Wang, and D. Jiang, *Existence and global attractivity of positive periodic solutions of periodic n-species Lotka-Volterra competition systems with several deviating arguments*, Math. Biosci., 160(1) (1999), 47–61.
- [15] M. S. Hashemi, E. Ashpazzadeh, M. Moharrami, and M. Lakestani, *Fractional order Alpert multiwavelets for discretizing delay fractional differential equation of pantograph type*, Appl. Numer. Math., 170 (2021), 1–13.
- [16] J. H. He, *Variational iteration method for autonomous ordinary differential systems*, Appl. Math. Comput., 114 (2000), 115–123.
- [17] C. S. Holling, *The components of predation as revealed by a study of small-mammal predation of the European pine sawfly*, Can. Entomol., 91(5) (1959), 293–320.
- [18] C. S. Holling, *The functional response of predators to prey density and its role in mimicry and population regulation*, Mem. Entomol. Soc. Can., 97(45) (1965), 5–60.
- [19] N. Khanna, V. Kumar, and S. K. Kaushik, *Vanishing moments of Hilbert transform of wavelets*, Poincare J. Anal. Appl., 2(2) (2015), 115–127.
- [20] N. Khanna, V. Kumar, and S. K. Kaushik, *Approximations using Hilbert transform of wavelets*, J. Classical Anal., 7(2) (2015), 83–91.
- [21] Y. Kuang, W. F. Fagan, and I. Loladze, *Biodiversity, habitat area, resource growth rate and interference competition*, Bull. Math. Biology, 65(3) (2003), 497–518.
- [22] A. Kumar, A. Khan, and A. Abdullah, *Fibonacci wavelet collocation method for solving dengue fever SIR model*, Mathematics, 12(16) (2024), Paper No. 2565, 14.
- [23] T. R. Malthus, *An essay on the principle of population*, 1st edition, 1798, 2nd edition in 1803, Introduction by Philip Appleman, and assorted commentary on Malthus edited by Appleman, Norton Critical Editions, 1798.
- [24] A. Moumen, A. Mennouni, and M. Bouye, *A Novel VietaFibonacci Projection Method for Solving a System of Fractional Integro-differential Equations*, Mathematics, 11(18) (2023), Paper No. 3985, 14.
- [25] N. A. Nayied, F. A. Shah, M. A. Khanday, and K. S. Nisar, *Numerical investigation of fractional order SEIR models with newborn immunization using Vieta-Fibonacci wavelets*, Partial Differ. Equ. Appl. Math., 12 (2024),



- Art. ID 100995, 17.
- [26] N. A. Nayied, F. A. Shah, K. S. Nisar, M. A. Khanday, and S. Habeeb, *Numerical assessment of the brain tumor growth model via Fibonacci and Haar wavelets*, *Fractals*, *31*(2) (2023), Art. ID 2340017, 17.
- [27] F. Nourian, M. Lakestani, S. Sabermahani, and Y. Ordokhani, *Touchard wavelet technique for solving time-fractional Black-Scholes model*, *Comput. Appl. Math.*, *41*(4) (2022), Paper No. 150, 19.
- [28] S. Olek, *An accurate solution to the multispecies Lotka-Volterra equations*, *SIAM Review*, *36*(3) (1994), 480–488.
- [29] C. Park, H. Rezaei, and M. H. Derakhshan, *An effective method for solving the multi time-fractional telegraph equation of distributed order based on the fractional order Gegenbauer wavelet*, *Appl. Comput. Math.*, *24*(1) (2025), 16–37.
- [30] R. A. Parker, *Feedback control of birth and death rates for optimal population density*, *Ecol. Model.*, *65*(1-2) (1993), 137–146.
- [31] S. Paul, S. P. Mondal, P. Bhattacharya, and K. Chaudhuri, *Some comparison of solutions by different numerical techniques on mathematical biology problem*, *Int. J. Differ. Equ.*, *2016*, Art. ID 8921710, 14.
- [32] S. Paul, S. P. Mondal, and P. Bhattacharya, *Numerical solution of Lotka Volterra prey predator model by using Runge-Kutta-Fehlberg method and Laplace Adomian decomposition method*, *Alex. Eng. J.*, *55*(1) (2016), 613–617.
- [33] K. T. Poumai, N. Khanna, and S. K. Kaushik, *Analysis of finite Haar wavelet transform and its implementation*, *Math. Methods Appl. Sci.*, *47*(18) (2024), 14431–14445.
- [34] C. Qiwu and G. J. Lawson, *Study on models of single populations: an expansion of the logistic and exponential equations*, *J. Theoret. Biol.*, *98*(4) (1982), 645–659.
- [35] P. Rahimkhani, Y. Ordokhani, and M. Razzaghi, *Fractional-order clique functions to solve left-sided Bessel fractional integro-differential equations*, *Chaos Solitons Fractals*, *14* (2025), Art. ID 101180, 9.
- [36] M. ur Rehman and R. A. Khan, *The Legendre wavelet method for solving fractional differential equations*, *Commun. Nonlinear Sci. Numer. Simul.*, *16*(11) (2011), 4163–4173.
- [37] K. Sadri, K. Hosseini, D. Baleanu, S. Salahshour, and C. Park, *Designing a Matrix Collocation Method for Fractional Delay Integro-Differential Equations with Weakly Singular Kernels Based on Vieta-Fibonacci Polynomials*, *Fractal Fract.*, *6*(1) (2022), Paper No. 2, 23.
- [38] J. K. Sahani, P. Kumar, and S. Sharma, *Computational study of white dwarfs and Lane-Emden type equations through Genocchi wavelet method*, *Int. J. Mod. Phys. C*, Art. ID 2550067, 22.
- [39] J. K. Sahani, P. Kumar, A. Kumar, and N. Khanna, *Numerical solution of non-linear Lienard equation using Haar wavelet method*, *Poincare J. Anal. Appl.*, *11*(2) (2024), 197–211.
- [40] M. Singh, S. Das, Rajeev and E. M. Craciun, *Numerical simulation of variable order fractional coupled Fitzhugh-Nagumo reaction-diffusion problem and its analysis*, *J. Appl. Anal. Comput.*, *15*(2) (2025), 810–838.
- [41] N. Yadav, A. Das, M. Singh, S. Singh, and J. Kumar, *Homotopy perturbation method and its convergence analysis for nonlinear collisional fragmentation equations*, *Proc. A.*, *479*(2279) (2023), Paper No. 20230567, 20.
- [42] J. K. Zhou, *Differential transformation and its applications for electrical circuits*, Huazhong Univ. Press, Wuhan, China, 1986.
- [43] L. Zou, Z. Zong and G. Dong, *Generalizing homotopy analysis method to solve Lotka-Volterra equation*, *Comput. Math. Appl.*, *56*(9) (2008), 2289–2293.

